The Astrophysical Journal, 598:162–167, 2003 November 20
© 2003. The American Astronomical Society. All rights reserved. Printed in U.S.A.

GALAXIES UNDER THE COSMIC MICROSCOPE: A GEMINI MULTIOBJECT SPECTROGRAPH STUDY OF LENSED DISK GALAXY 289 IN A2218

A. M. Swinbank,[1] J. Smith,[2] R. G. Bower,[1] A. Bunker,[2] I. Smail,[1] R. S. Ellis,[3] Graham P. Smith,[1,3] J.-P. Kneib,[3,4] M. Sullivan,[1] and J. Allington-Smith[1]

Received 2003 April 10; accepted 2003 July 30

ABSTRACT

In this paper, we exploit the gravitational potential of the rich cluster A2218 as a magnifying glass. We demonstrate that the magnification due to the cluster allows us to observe distant background galaxies at a comparable level of detail to galaxies at $z \sim 0.1$. Using the Gemini Multiobject Spectrograph (GMOS) integral field unit (IFU) on Gemini North, we observed the spatially resolved [O II] λ3727 emission line spectrum for a lensed disk galaxy at $z = 1.034$. Using a detailed model for the cluster mass distribution, we are able to correct for the lensing by the cluster and reconstruct the source morphology. We find that the overall magnification is a factor of 4.92 ± 0.15, and the rest-frame absolute I-band magnitude is $M_I^{\rm rest} = -22.4 \pm 0.2$, where the error bars include conservative estimates of the uncertainty in the source-plane reconstruction. The inclination-corrected circular velocity is 206 ± 18 km s^{-1}. The galaxy lies very close to the mean Tully-Fisher relation of present-day spirals. Although our results are based on a single object, they demonstrate that gravitational lensing can be viably used to make detailed studies of the evolution of the structure of distant field galaxies.

Subject headings: galaxies: evolution — galaxies: formation — galaxies: halos — galaxies: high-redshift — galaxies: kinematics and dynamics — galaxies: spiral

1. INTRODUCTION

The deflection of light rays by the deep gravitational potential of galaxy clusters can be harnessed to greatly increase the effective collecting area of astronomical telescopes. Such "gravitational telescopes" magnify the images of background objects, allowing us to study faint distant galaxies in a level of detail that would simply not be possible by conventional means (Smail et al. 1996; Franx et al. 1997; Teplitz et al. 2000; Ellis et al. 2001; Campusano et al. 2001; Smith et al. 2002). In particular, many of the selection biases that require us to observe only bright, extended galaxies are removed, allowing us to test models for galaxy formation in a much fairer way than otherwise possible.

In this paper, we will concentrate on the dynamics of galaxies seen at $z \sim 1$ by measuring the rotation speeds of gas in these systems through the [O II] λ3727 emission line. By observing the distant ($z > 1$) universe, we sample cosmic history at a time before many present-day stars had formed. The "classical" galaxy formation model, in which the formation of a dark halo precedes the formation of the galaxy's disk (with the disk subsequently growing over an extended period of time through the gradual accretion of gas from the halo; e.g., Eggen, Lynden-Bell, & Sandage 1962; Larsen et al. 1980; Sandage 1990), predicts that the stellar masses at a given circular velocity will be much lower at $z = 1$ (by about a factor of 2) than at the present day. In contrast, CDM hierarchical models predict that galaxies would follow a similar stellar mass versus circular velocity correlation at all redshifts. Previous work in this area has, by necessity, concentrated on galaxies that are intrinsically bright and mostly at $z < 0.5$ (Vogt et al. 1997; Verheijen 2001; Böhm, Ziegler, & Fricke 2003; Ziegler et al. 2003), with only a few galaxies being studied at higher redshift (Vogt et al. 1996; Milvang-Jensen et al. 2003; Barden et al. 2003). The results suggest an increase in B-band luminosity for a given circular velocity (Vogt & Phillips 2002; Kannappan, Fabricant, & Franx 2002), suggesting a preference for hierarchical formation models.

Here we demonstrate the feasibility of using lensing to study the evolution of the Tully-Fisher relation at much higher redshift. We use the Gemini Multiobject Spectrometer (GMOS) integral field unit (IFU) on Gemini North to target the gravitationally lensed $z = 1.034$ arc (object 289)—we use the same numbering system as Pelló et al. (1992) in cluster A2218. We use a cosmology with $H_0 = 75$ km s^{-1} Mpc^{-1} and $q_0 = 0.05$, to be consistent with Vogt et al. (1997). We note that for a cosmology with $\Omega_M = 0.3$ and $\Omega_\Lambda = 0.7$, the results are very similar: the physical distances are only 6% larger and the luminosities 12% brighter.

2. OBSERVATIONS, ANALYSIS, AND RESULTS

The galaxies lensed by the A2218 cluster were first studied by Pelló et al. (1988), and later a number of arcs and arclets were discovered in the cluster core (Kneib et al. 1996; Ebbels et al. 1998; Ellis et al. 2001). Spectroscopy of the arcs in the cluster have confirmed a redshift for arc 289 of 1.034 (Pelló et al. 1992; Ebbels et al. 1998).

2.1. *HST Observations and Lens Model*

The cluster was first observed by the *Hubble Space Telescope* (*HST*) WFPC2 in 1994 September in the R_{702} filter for a total of 6.4 ks (see Kneib et al. 1996). It was subsequently observed again in 2000 January using the B_{450}, V_{606}, and I_{814} filters for totals of 12.0, 10.0, and 12.0 ks, respectively (discussed in Smail et al. 2001).[5]

[1] Department of Physics, University of Durham, South Road, Durham DH1 3LE, UK; a.m.swinbank@dur.ac.uk.
[2] Institute of Astronomy, University of Cambridge, Madingley Road, Cambridge CB3 0HA, UK.
[3] California Institute of Technology, MC 105-24, Pasadena, CA 91125.
[4] Observatoire Midi-Pyrénées, 14 Avenue East Belin, 31400 Toulouse, France.

[5] Based on observations made with the NASA/ESA *Hubble Space Telescope*, which is operated by STSCI for the Association of Universities for Research in Astronomy, Inc., under NASA contract NAS5-26555.

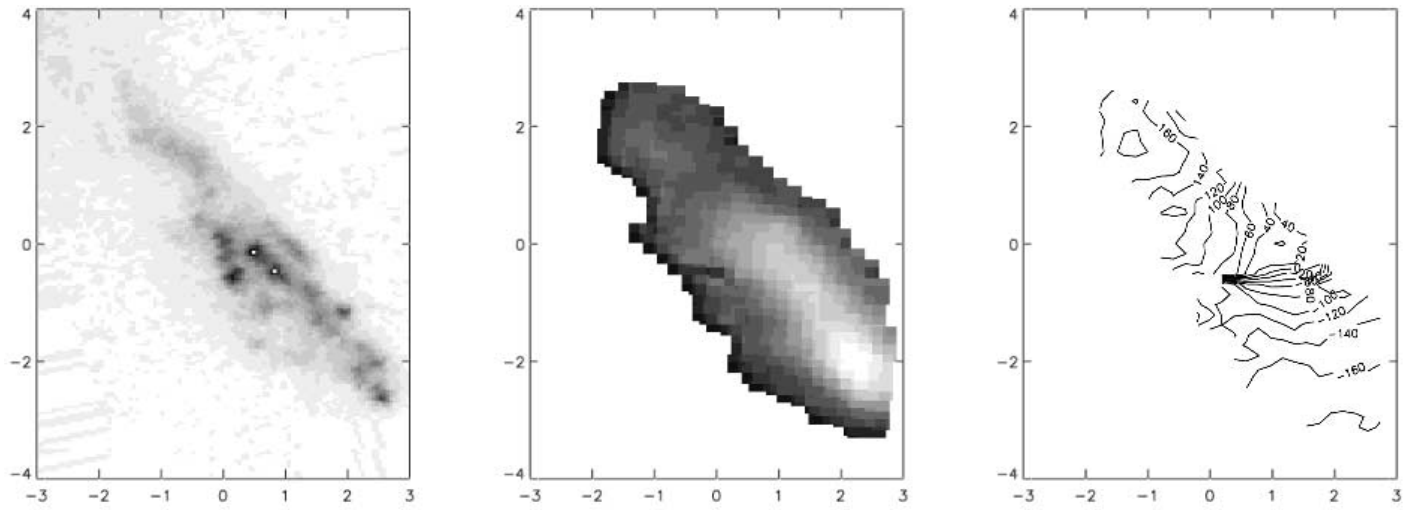

FIG. 1.—*Left*: Arc 289 in A2218, generated by combining the *HST* WFPC2 B_{450}, V_{606}, and I_{814} drizzled images. *Middle*: [O II] λ3727 emission map of the arc measured from our IFU observations. The distribution of [O II] emission agrees well with the UV flux seen in the left panel (the seeing for the observations was 0.″7). *Right*: Contour map of the derived velocity field of the galaxy. The scale is marked in arcseconds. North is up and east is left.

Arc 289 is a fairly blue disk galaxy at $\alpha = 16^{h}35^{m}55^{s}.1$, $\delta = +66°11'51''.0$ (J2000), lying in a saddle between the central dominant galaxy of the cluster (301) and a subclump of elliptical galaxies (307 and 292; Fig. 1 in Smail et al. 2001). The *HST* images of the galaxy show a large amount of internal structure with the knotted, disklike morphology resembling a late-type galaxy (especially the *B*-band flux, which samples the rest-frame UV and is therefore dominated by the star-forming H II regions; Fig. 1, *left*). We calculate the magnitude of the arc in various passbands in Table 1 by using the IRAF *imsurfit* package, with the sky estimated from a second-order polynomial surface fit to regions around the galaxy. We then use SExtractor (Bertin & Arnaud 1996) to estimate the residual background within the frame.

To correct for the distortion and magnification of the galaxy image by the cluster lens, we need to employ a lens model. A detailed mass model for A2218 was originally developed by Kneib et al. (1996) from *HST* imaging, and this has been updated by Ellis et al. (2001) and Smith et al. (2003). In particular, Smith (2002; Smith et al. 2003) incorporated all of the strong lensing constraints to produce one of the best-constrained strong lensing clusters, with three spectroscopically confirmed multiple-image systems. The precision of this lens model makes this cluster and ideal gravitational telescope with which to study (and reconstruct) the detailed properties of high-redshift galaxies.

TABLE 1
OBSERVATION RESULTS

Filter	Magnitude	b/a	Inclination (deg)
B_{450}	21.66 ± 0.04	0.37	68
V_{606}	20.86 ± 0.10	0.41	66
R_{702}	20.53 ± 0.04	0.40	66
I_{814}	19.79 ± 0.05	0.53	58
J	18.63 ± 0.06	...	...
K	17.32 ± 0.06	...	...
IFU	...	0.5184	58

NOTES.—Aperture magnitudes of the arc are in the Vega-based system. Inclination is computed in the source (reconstructed) frame.

While the giant blue arc 289 is highly distorted at the northern end (Fig. 1*a*), extending across the halo of the cluster galaxy 244, the majority of the source lies outside the caustic, producing a highly magnified, weakly sheared image. The southern end of the arc does not suffer the same strong shear and is not so distorted, although it has a higher surface brightness than the northern end. Exploiting the fact that gravitational lensing conserves surface brightness, we compute the magnification in each band by using the transformation between the sky-plane and source-plane coordinates and compare the flux in the (reconstructed) source and (observed) sky frames (Fig. 2, *left*). We use Smith's (2002) model of A2218 to compute the magnification (μ) of 289, obtaining a mean luminosity-weighted magnification of $\mu = 4.92$ across the whole galaxy image. The spatial variation of surface brightnesses may vary between filters because of differing spatial distributions of stellar populations (and dust) in the lensed galaxy, thus causing the magnification to vary by ± 0.15, depending on the band. The statistical error bar on μ is derived from the family of lens models that adequately reproduce the multiply imaged arcs in the cluster. We estimate the 1 σ uncertainty by perturbing the parameters of the best-fit lens model such that $\Delta\chi^2 = 1$. For each model, we recompute the magnification of 289. The error corresponds to the largest variation in magnification that we found and is converted into a conservative estimate of ± 0.05 mag in the source-plane photometry of 289.

2.2. *Ground-Based Imaging*

Additional constraints on the spectral energy distribution (SED) of the galaxy comes from the near-infrared imaging of this field using the INGRID camera (Packham et al. 2003) on the William Herschel Telescope.[6] The reduction and analysis of these data is described by Smail et al. (2001).

[6] Based on observations made with the William Herschel Telescope, operated on the island of La Palma by the Isaac Newton Group in the Spanish Observatorio del Roque de los Muchachos of the Instituto de Astrofisica de Canarias.

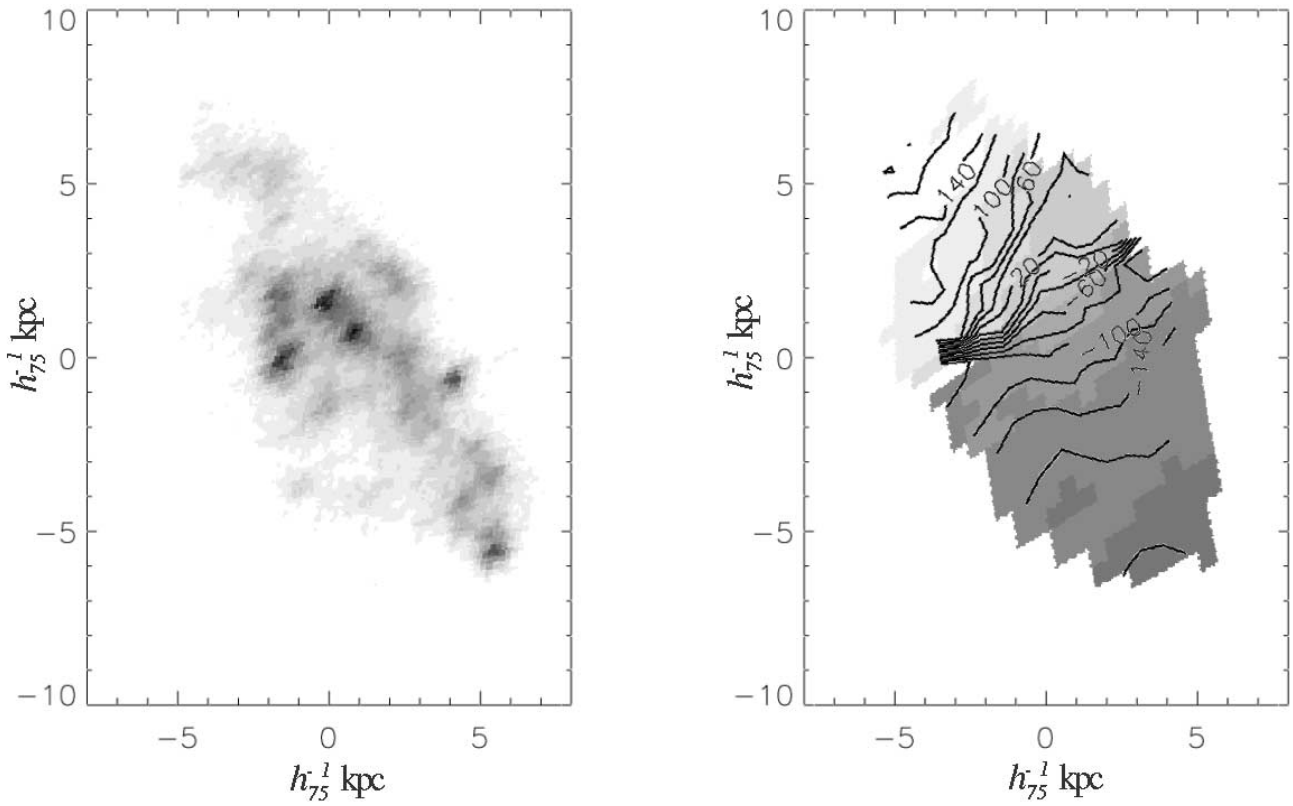

FIG. 2.—Reconstructed image of the arc corrected for lens magnification using the mass model of Smith et al. (2003). *Left*: Reconstructed image of the galaxy based on *HST* imaging. *Right*: Velocity map of the galaxy in the source frame. The dark and light regions represent redshift and blueshift, respectively, and the contours map the velocity in the source plane. The luminosity-weighted magnification of the source is 4.92 ± 0.15 but varies from ~5.6 to ~4.9 from the northern to southern end of the arc. The scale shows the size of the galaxy in the source frame. Without a lens, at $z = 1$, 1″ corresponds to 7.7 kpc.

With our multiwavelength photometry (Table 1), we construct an SED of this very blue galaxy, whose colors indicate a current-to-past star formation rate consistent with that seen for late-type spirals at the present day. The rest-frame *I*-band luminosity is approximately equivalent to the observed *H*-band and so is calculated from the *J* and *K* photometry (Table 1). We co-add the *J*, *K* images to obtain an aperture which is used to extract the *J*, *K* magnitudes and interpolate for the relevant SED type. We derive a rest-frame *I*-band magnitude of $M_I = -24.1 \pm 0.1$. Correcting for the magnification due to the lens, the absolute rest-frame *I*-band magnitude is $M_I^{\rm rest} = -22.4 \pm 0.2$. We apply the same technique for the rest-frame *B*-band magnitude (at $z \sim 1$, *I* and *R* bands are the closest match to rest-frame *B* band) and estimate its uncertainty by computing the magnitude for a variety of SED types that are consistent with the observed optical colors. We compute a corrected rest-frame *B*-band magnitude of $M_B^{\rm rest} = -21.1 \pm 0.2$. Accounting for the $(1+z)^4$ dimming, the central surface brightness of the galaxy ($\mu_{b,0} \sim 20.6$) confirms 289 as a high surface brightness galaxy.

The inclination is determined by transforming the *HST* images of the galaxy to the source plane. We fit ellipses to an isophote of the galaxy image in the source plane using the IDL *gauss2dfit* routine. The ellipticity is then $e = 1 - b/a$ (where *a* and *b* are the major and minor axis of the ellipse) and the inclination, *i*, is $\cos i = b/a$. The average axis ratio of the ellipses in the four passbands (Table 1) is 0.43 ± 0.07, which translates to an inclination of $64^\circ \pm 6^\circ$, assuming an intrinsically circular disk.

2.3. *GMOS Spectroscopic Imaging*

A2218 arc 289 was observed with the GMOS-IFU on Gemini North on 2002 June 12 UT during science demonstration time for a total of 5.4 ks in 0.″7 seeing and photometric conditions. The IFU uses a lensed fiber system to reformat the $7'' \times 5''$ field into two long slits (Allington-Smith et al. 2002). Using an *I*-band filter in conjunction with the R400 grating results in two tiers of spectra recording a maximum field of view. The spectral resolution of this configuration is $\lambda/\Delta\lambda = 2000$. For the galaxy at $z = 1.034$, the emission for the [O II] doublet falls at a wavelength of 7581 Å, in a region of low sky emission.

The GMOS data reduction pipeline was used to extract and wavelength calibrate the spectra of each IFU element. The variations in fiber-to-fiber response were removed in IDL by using continuum regions either side of the expected range of [O II] emission. The [O II] doublet is clearly resolved in the GMOS spectra (Fig. 3). This is useful, since one of the [O II] lines can clearly be identified even when the other lies immediately under the narrow sky line at ~7580 Å. The emission line doublet was fitted using a χ^2 minimization procedure, taking into account the greater noise at the position of the sky line. The spectra were averaged over a 3×3 spatial pixel region, increasing this region to 4×4 pixels if the signal was too low to give a sufficiently high χ^2 improvement over a fit without the line. In regions where this averaging process still failed to give an adequate χ^2, no fit was made. With a continuum fit we required a minimum χ^2 of 25 (S/N of 5) to detect the line. To compute the error, the

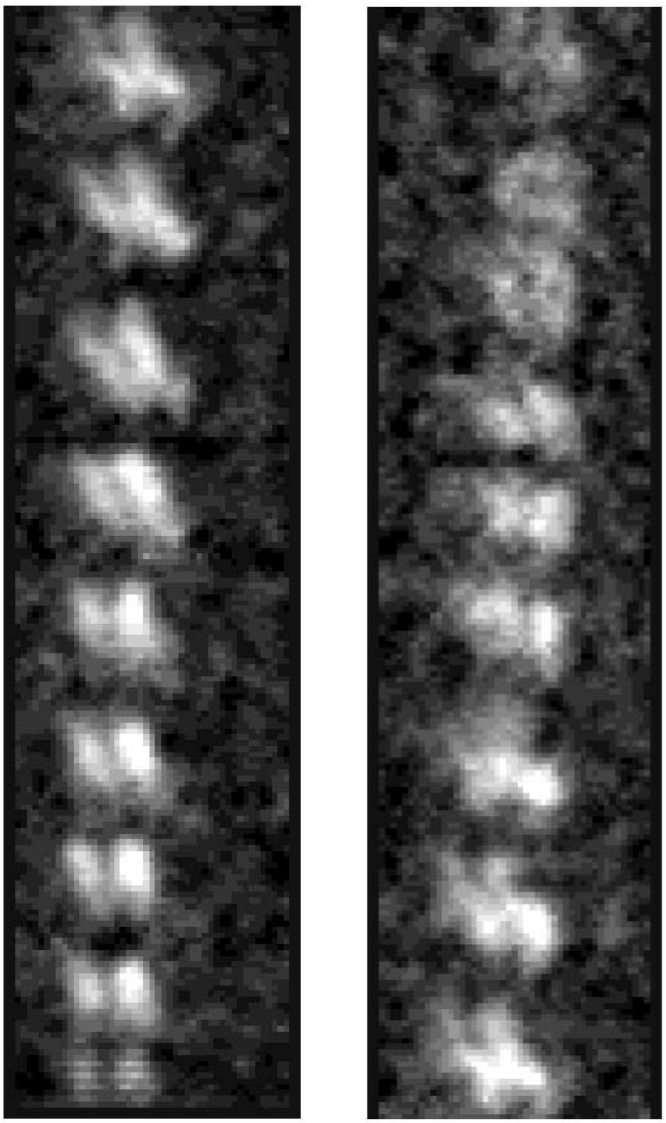

FIG. 3.—Examples of the [O II] emission doublet as seen in the reduced IFU data. Each line of the image is the spectrum from a single IFU lenslet. These are arranged in blocks: each block corresponds to an east-west slice through the short dimension of the galaxy. The rotation of the galaxy can be seen in each block as well as between blocks, clearly showing that the lensed galaxy's dynamics are resolved in both dimensions.

velocity parameter of the best-fit line is varied until the signal drops by a χ^2 of 9. The range in velocity corresponds to a formal 3 σ error.

We use the velocity field to infer the rotational velocity of the galaxy's gas disk. As can be seen from the major axis cross section (Fig. 4, *inset*), the asymptotic rotation speed is $v_{\rm rot} = 186 \pm 16$ km s^{-1} (i.e., the total velocity shift across the galaxy is $2v_{\rm rot}$). The inclination-corrected velocity of the galaxy is 206 ± 17 km s^{-1}. This corresponds to a dynamic mass of $1.4 \times 10^{11}\ M_\odot\ h_{75}^{-1}$ within a radius $\sim$14 h_{75}^{-1} kpc in this cosmology.

In addition, the shape of the rotation curve can be compared to the low-redshift ($z \sim 0.03$) sample of spiral galaxies by Courteau (1997). We fit the observed source plane one-dimensional rotation curve by convolving the arctan and multiparameter models (Courteau 1997) with 0.″7 seeing (transformed to the source plane). When we use a χ^2 fit, the observed rotation curve is best described with an arctan function with transition radius, $r_t = 1.7$ kpc (where r_t describes the transition radius between the rising and flattening of the curve) or a multiparameter fit with $r_t = 2.1$ kpc, $\gamma = 1.5$. To compare the shape of the rotation curve with Courteau's sample, we compute $r_t/r_{\rm opt}$ (where $r_{\rm opt}$ is the radius enclosing 83% of the light in the source-plane photometry) to be $\sim$0.25. This ratio is higher than most galaxies in the local sample but not anomalous. Around 10% of local bright galaxies have similarly shaped rotation curves.

3. DISCUSSION

The tight correlation between luminosity and rotation velocity for spiral galaxies in the local universe is known as the Tully-Fisher (TF) relation (Tully & Fisher 1977). With a single high-redshift galaxy, we can measure the evolution of the offset in the TF relation under the assumption that the slope remains fixed. In Figure 4, we compare the rotation velocity and source brightness of arc 289 with that of local and other high-redshift galaxies in rest frames *B* and *I*. While the current high-redshift data are concentrated in rest-frame *B*-band, rest-frame *I*-band observations will prove a more rigorous test of evolution of the TF relation, since the corrections for dust and ongoing star formation are much smaller at longer wavelengths. The rest-frame *I*-band TF therefore gives a clearer indication of the true stellar luminosity and, hence, the ratio of stellar mass to total halo mass.

The position of the galaxy on the TF relation in both the *B* and *I* bands shows good agreement with local data (Pierce & Tully 1992; Mathewson, Ford, & Buchhorn 1992; Haynes et al. 1999; Tully & Pierce 2000; Verheijen 2001). The galaxy is slightly offset to brighter magnitudes in the *B*-band relation, as we would expect from its blue colors. These data are in agreement with existing intermediate ($z \sim 0.5$; Vogt et al. 1997; Milvang-Jensen et al. 2003; Böhm et al. 2003; Ziegler et al. 2003) and high-redshift studies ($z \sim 1$; Vogt & Phillips 2002; Barden et al. 2003). It should be noted, however, that these studies generally have to infer the turnover in the rotation curve from deconvolution of the rising rotation speed and the seeing. This might lead to a systematic underestimate of the asymptotic rotation speed. In contrast, our data clearly resolve the shape of the rotation curve (Fig. 4, *inset*), leading to much smaller uncertainty in the rotation speed of an individual galaxy.

Clearly, it would be dangerous to draw far-reaching conclusions from a single galaxy, but the following comparison illustrates the sensitivity that can be expected if this level of evolution is confirmed by further observations. The theoretical evolution of the *I*-band TF relation from hierarchical models of galaxy formation from Cole et al. (2000) predict that for any given disk circular velocity, the *I*-band luminosity should decrease by $\sim$0.1 mag from $z = 0$ to 1, while in the *B* band, such models predict an increase in luminosity of $\sim$0.5 mag for the same redshift change. In contrast, we would expect a decrease in luminosity of $\sim$0.7 mag from $z = 0$ to 1 if all of the galaxy's mass were already in place at $z = 1$, but only half of the stars had yet formed. The small change in the *I*-band magnitude shown by arc 289 suggests a preference for the hierarchical rather than the "classical" formation model.

The methods we have developed in this paper show the potential of IFU observations of gravitational lensed

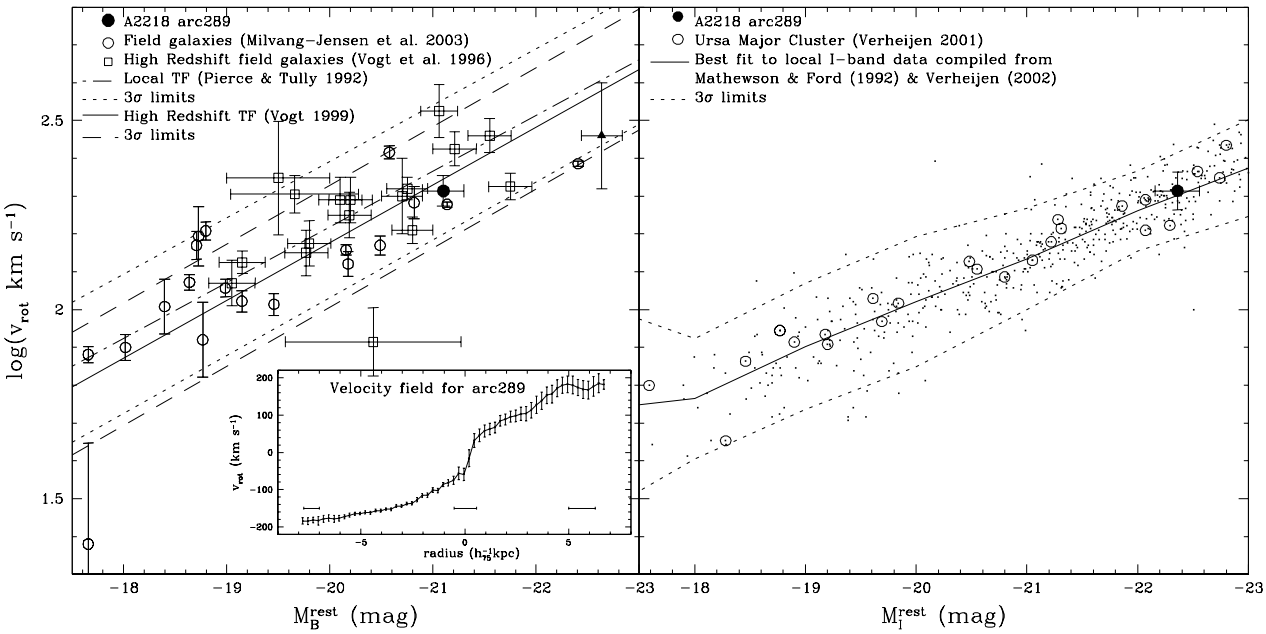

FIG. 4.—*Left*: Arc 289 on the Tully-Fisher relation in rest-frame *B* band compared to high-redshift ($z \sim 0.83$) field galaxies (Milvang-Jensen et al. 2003) and the high-redshift sample from Vogt (1999). For comparison, we show the low redshift local fit from Pierce & Tully (1992). *Solid triangle*: Massive disk galaxy L451 at $z = 1.34$ (van Dokkum & Stanford 2001). The galaxy rotation curve (*inset*) shows the peak-to-peak rotation velocity of the arc in [O II] emission built from the IFU image in the source plane. The error bars shown are formally 3 σ, and alternate points are independent. The horizontal error bars show 0.″7 seeing transformed to the source plane. *Right*: Rest-frame *I*-band Tully-Fisher relation compiled from Mathewson, Ford, & Buchhorn (1992) and from the Ursa Major Cluster (Verheijen 2001). *Solid point*: Arc 289, lying very close to the mean Tully-Fisher relation for present-day spirals. The small change in the *I*-band magnitude shown by Arc 289 suggests a preference for hierarchical rather than the classical formation model.

galaxies as a means of studying the spatially resolved properties of high-redshift galaxies in a remarkable level of detail. While we have concentrated here on the dynamics of the galaxy 289 in A2218, our data can also be used to investigate the spatial distribution of star formation. By combining these optical data with observations with near-infrared IFUs, it will be possible to study the emission line ratios of [O II]:[O III] and Hα:Hβ. We could then determine the distribution of reddening across the galaxy and its spatially resolved chemical abundance. This would provide powerful insight into the nature of star-forming galaxies at this early epoch.

This work is based on observations obtained at the Gemini Observatory, which is operated by the Association of Universities for Research in Astronomy, Inc., under a cooperative agreement with the NSF on behalf of the Gemini partnership: the National Science Foundation (United States), the Particle Physics and Astronomy Research Council (United Kingdom), the National Research Council (Canada), CONICYT (Chile), the Australian Research Council (Australia), CNPq (Brazil), and CONICET (Argentina). We would like to thank Matt Mountain for accepting this program for GMOS IFU Science Demonstration. We thank Inger Jørgensen, Matt Mountain, Jean Rene-Roy, Kathy Roth, Marianne Takamiya, Roger Davies, Gerry Gilmore, Bryan Miller, Chris Packman, Bo Milvang-Jensen, Carlton Baugh, David Gilank, Nathan Courtney, and Richard McDermid for their vital assistance with the planning, preperations, observations, and discussion, and Robert Content and Graham Murray for designing and building the instrument. A. M. S. acknowledges the support of a PPARC postgraduate studentship, R. G. B. acknowledges support from the Leverhulme Trust and Euro 3D Research Training Network, and I. R. S. acknowledges support from the Royal Society and the Leverhulme Trust.

REFERENCES

Allington-Smith, J. R., et al. 2002, PASP, 114, 892
Barden, M., Lehnert, M. D., Tacconi, L., Genzel, R., White, S., & Franceschini, A. 2003, ApJ, submitted (astro-ph/0302392)
Bertin, E., & Arnaud, S. 1996, A&AS, 117, 393
Böhm, A., Ziegler, B. L., & Fricke, K. J. 2003, Astrophys. Space Sci., 284, 689
Campusano, L. E., Pelló, R., Kneib, J.-P., Le Borgne, J.-F., Fort, B., Ellis, R., Mellier, Y., & Smail, I. 2001, A&A, 378, 394
Cole, S., Lacey, C., G., Baugh, C. M., & Frenk, C. S. 2000, MNRAS, 319, 168
Courteau, S. 1997, AJ, 114, 240
Ebbels, T., Ellis, R., Kneib, J. P., Leborgne, J. F., Pelló, R., Smail, I., & Sanahuja, B. 1998, MNRAS, 295, 75
Eggen, O. J., Lynden-Bell, D., & Sandage, A. R. 1962, ApJ, 136, 748
Ellis, R., Santos, M. R., Kneib, J. P., & Kuijken, K. 2001, ApJ, 560, L119
Franx, M., Illingworth, G. D., Kelson, D. D., van Dokkum, P. G., & Tran, K. 1997, ApJ, 468, L75
Haynes, M. P., Giovanelli, R., Salzer, J. J., Wegner, G., Freudling, W., da Costa, L. N., Herter, T., & Vogt, N. P. 1999, ApJ, 117, 1668
Kannappan, S. J., Fabricant, D. G., & Franx, M. 2002, AJ, 123, 2358
Kneib, J. P., Ellis, R., Smail, I., Couch, W. J., & Sharples, R. M. 1996, ApJ, 471, 643
Larson, R. B., Tinsley, B. M., & Caldwell, C. N. 1980, ApJ, 237, 692
Mathewson, D. S., Ford, V. L., & Buchhorn, M. 1992, ApJS, 81, 413
Milvang-Jensen, B., Aragón-Salamanca, A., Hau, G. K. T., Jørgensen, I., & Hjorth, J. 2003, MNRAS, 339, 1
Packham, C., et al. 2003, MNRAS, submitted
Pelló, R., Le Borgne, J. F., Sanahuja, B., Mathez, G., & Fort, B. 1988, A&A, 190, L11
———. 1992, A&A, 266, 6
Pierce, M. J., & Tully, R. B. 1992, ApJ, 387, 47

Sandage, A. 1990, J. Royal Astron. Soc. Canada, 84, 70
Smail, I., Dressler, A., Kneib, J. P., Ellis, R. S., Couch, J. W., Sharples, R. M., & Oemler, A. 1996, ApJS, 459, 508
Smail, I., Kuntschner, H., Kodama, T., Smith, Graham P., Packham, C., Fruchter, A. S., & Hook, R. N. 2001, MNRAS, 323, 849
Smith, G. P. 2002, Ph.D. thesis, University of Durham, UK
Smith, G. P., Edge, A. C., Eke, V. R., Nichol, R. C., Smail, I., & Kneib, J.-P. 2003, ApJ, 590, L79
Smith, G. P., Smail, I., Kneib, J.-P., Davis, C. J., Takamiya, M., Ebeling, H., & Czoske, O. 2002, MNRAS, 333, L16
Teplitz, H. I., et al. 2000, ApJ, 533, L65
Tully, R. B., & Fisher, J. R. 1977, A&A, 54, 661
Tully, R. B., & Pierce, M. J. 2000, ApJ, 533, 744
van Dokkum, P. G., & Stanford, S. A. 2001, ApJ, 562, L35
Verheijen, M. A. W. 2001, ApJ, 563, 694
Vogt, N. P. 1999, in ASP Conf. Proc. 193, Hy-Redshift Universe: Galaxy Formation and Evolution at High Redshift, ed. A. Bunker & W. van Breugel (San Francisco: ASP), 145
Vogt, N. P., Forbes, D. A., Phillips, A. C., Gronwall, C., Faber, S. M., Illingworth, G. D., & Koo, D. C. 1996, ApJ, 465, L15
Vogt, N. P., & Phillips, A. C. 2002, A&AS, 200, 4008
Vogt, N. P., et al. 1997, ApJ, 479, 121
Ziegler, B. L., Bohm, A., Jager, K., Fritz, A., & Heidt, J. 2003, preprint (astro-ph/0303417)